Process Safety and Environmental Protection 164 (2022) 1–14

Contents lists available at ScienceDirect

Process Safety and Environmental Protection

journal homepage: www.journals.elsevier.com/process-safety-and-environmental-protection

Simultaneous optimization of economic, environmental and safety criteria for algal biodiesel process retrofitted using dividing wall column and multistage vapor recompression

Gunavant Deshpande [a], Savyasachi Shrikhande [b], Dipesh S. Patle [a], Ashish N. Sawarkar [a,*,1]

[a] Department of Chemical Engineering, Motilal Nehru National Institute of Technology Allahabad, Prayagraj 211 004, Uttar Pradesh, India
[b] Chemical Engineering and Analytical Science, University of Manchester, Manchester M13 9PY, United Kingdom

ARTICLE INFO

Keywords:
Multiobjective optimization
Microalgal biodiesel
In situ
Ultrasound assisted
Divided wall column
Multistage vapor recompression

ABSTRACT

The present study deals with the multiobjective optimization (MOO) of retrofitted in situ algal biodiesel process. Transesterification of the algal lipids is intensified using ultrasonication and catalyzed using the ionic liquid catalyst. Process includes the retrofitting of two conventional distillation columns into a dividing wall column (DWC), which is further intensified using multistage vapor recompression (DWC-MVR) in order to decrease the energy consumption and CO_2 emission from the process. Excel based hybridised multiobjective differential evolutionary dynamic local search (HMODE-DLS) algorithm is used for the constrained MOO, whereas Aspen Plus is used for the process development. Break even cost (BEC), eco indicator (EI99) and individual risk (IR) are considered as objectives to evaluate economic, environmental impact, and safety of process, respectively. Initially, bi-objective case studies were analyzed and finally, all three objectives are studied in one case. Pareto optimal solutions obtained from HMODE-DLS algorithm are then ranked by the simple additive weighted method to find out the best solution. MOO resulted in the significant decrease in BEC (~20%), EI99 (~48%) and IR (~10%).

1. Introduction

Progressive exhaustion of fossil fuel resources, increase in environmental cognizance, and the notable rise in fossil fuel prices have demanded the search of fuels from renewable sources (Sivaramakrishnan and Muthukumar, 2012). Biodiesel has sparked interest as a possible replacement for fossil energy, and is seen as a significant step forward in reducing greenhouse gas emissions and minimizing air pollution (Akkarawatkhoosith et al., 2019; Mathew et al., 2021; Pukale et al., 2015). Transesterification is the key reaction in the transformation of bio-oil into biodiesel. Conventionally, biodiesel synthesis is carried out in two steps, viz. oil extraction and its transesterification. Oil extraction and its transesterification are simultaneously carried out in an in situ process, thereby decreasing the footprint and potentially reducing the capital investment as well as the costs associated with heating/-stirring (Ayub et al., 2022; Gunawan et al., 2014; Patle et al., 2021;

Abbreviations: BMC, Bare module cost; BBAIL, Benzimidazolium based Bronsted Acid Ionic Liquid; BEC, Breakeven cost; CEPCI, Chemical engineering plant cost index; COMP2-CR, Compression ratio of compressor 2; COM, Cost of manufacturing; DWC, Dividing wall column; DLS, Dynamic local search; DWC-MVR, Dividing wall column with multistage vapor recompression; DAG, Diacetin; EI99, Eco indicator; f_i, Occurrence frequency of i^{th} incident; HMODE-DLS, Hybridised multiobjective differential evolutionary dynamic local search; IR, Individual risk; IL, Ionic liquid; LC_{50}, Median fatal concentration; LFL, Lower flammability limit; LIQ-SPLIT-F4, Liquid split on either side of the wall in DWC; MAG, Monoacetin; MOO, Multiobjective optimization; MODE, Multiobjective differential evolutionary; MVR, Multistage vapor recompression; NSGA II, Non-dominated sorting genetic algorithm; NRTL, Non-random two-liquid; OH-VAP-SPLIT, Overhead vapor split; $P_{x,y}$, Probability of injury or decease caused by i^{th} incident; Q, Population size; QRA, Quantitative risk analysis; SAW, Simple Additive Weighting; TAG, Triacetin; TMC, Total module cost; TAC, Total annual cost; UFL, Upper flammability limit; UNIFAC, UNIQUAC Functional-group Activity Coefficients; V, Causative variable (dose, thermal radiation, overpressure); VAP-SPLIT-F3, Vapor split into either side of the wall in DWC; Y, Probit function; δ_d, normalisation factor for damage in category d; ω_d, damage weighting factor for category d; β_b, amount of chemical b released by direct emission per unit of reference; $\alpha_{b,k}$, damage in category k per unit of chemical b released to the environment.

* Corresponding author.
E-mail address: ansawarkar@mnnit.ac.in (A.N. Sawarkar).
[1] ORCID ID:0000-0003-1772-7938

https://doi.org/10.1016/j.psep.2022.05.059
Received 17 March 2022; Received in revised form 8 May 2022; Accepted 24 May 2022
Available online 27 May 2022

Suganya et al., 2014).

Biodiesel obtained from first and second generation feedstocks (mainly comprising of edible oils) were unable to establish themselves as a sustainable source due to their direct influence on the food chain (Christophe et al., 2012; Deshmukh et al., 2019). Microalgae, yeast, and fungi are oleaginous microbes that are proposed as a third-generation feedstock(Ahmed et al., 2020). Out of the proposed sources, microalgae biodiesel was discovered to be a practical alternative for rising fuel demand(Alagumalai et al., 2021; Chisti, 2008). The high photosynthetic efficiency of microalgae, ability to fix CO_2, and ability to be cultivated on non-agriculture land (Deshmukh et al., 2019; Rastogi et al., 2018), make the microalgae an attractive choice for biodiesel synthesis. As reported by Milbrandt and Jarvis (2010), wasteland in India can produce on average 7 ton of lipid per hector. In order to provide 50322 kg/h of lipid 402.5 ton of lipid is required per year. Hence, to produce 402.5 ton of lipid 57510 hectors of land is required. India has around 55237 thousand of hectors of waste land on which conventional farming is not possible and this land can be used for the microalgae cultivation. Therefore, continuous feed of lipid for the biodiesel plant is feasible in India. Currently microalgal biodiesel is not economically appealing, due to its high cost of production, that is largely dependent of high water content of the biomass and separation difficulties (Mustapha et al., 2021). Development of suitable catalyst (Ganesan et al., 2021), improvements in algal cultivation (Ananthi et al., 2021), and optimal process design can help in minimizing the cost of biodiesel production.

Ionic liquid (IL) catalyzed biodiesel synthesis has recently emerged as a possible avenue to an environmentally friendly biodiesel production (Ong et al., 2021). IL catalyzed reactions have been shown to have excellent reactivity under mild conditions and high selectivity for the ester product with easy separations (Patle et al., 2020; Barange et al., 2021). Benzimidazolium based Bronsted Acid Ionic Liquid (BBAIL) depicted 96% conversion for biodiesel production (Khiratkar et al., 2018). BBAIL catalyst is also useful in the presence of ultrasound intensification for the transesterification reaction and can be recycle effectively three times (Patle et al., 2018). Conventional acid and base catalyst, such as NaOH, H_2SO_4, KOH, HCL has been intensively used for the transesterification. But the presence of free fatty acid and water in the lipids limit the utilization of these catalyst. Their harmful and non-green properties make them unsustainable to the environment (Ong et al., 2021). Also, lower yield and separation cost of the catalyst increase the operation cost of the biodiesel (Sivaramakrishnan and Incharoensakdi, 2017). Some heterogenous catalysts developed by the researchers have shown higher yield, but the recyclability is the main limitation for the use of such heterogenous catalysts. Heterogeneous catalysts lose activity after some uses, and disposal of the used heterogeneous catalysts is also a major environmental concern. Ionic liquid catalysts are easy to recycle and their activity remains unaltered even after multiple usages. Bronsted acidic ILs can convert free fatty acids and triglycerides into biodiesel without pre-treatment and in turn, lowers the biodiesel production cost (Ong et al., 2021).

Retrofitting is being increasingly explored to increase the efficiency of the existing chemical plant in term of economics, CO_2 emission, waste minimisation, capacity expansion etc. Divided wall column (DWC) is utilised for ternary separations, which involve implanting a vertical wall in a column to separate column into two portions. Technoeconomic viability of the biodiesel process from microalgae was reported by various researchers (Deshpande et al., 2022; Heo et al., 2019; Patle et al., 2020; Shrikhande et al., 2021). Shrikhande et al. (2021) proposed the retrofitted divided wall column with multistage vapor recompression (DWC-MVR) process for an in-situ biodiesel production. DWC-MVR can result in significant saving in energy in the distillation systems. Multistage vapor recompression (MVR) is useful even for wide boiling mixture as opposed to simple vapor recompression (Kumar et al., 2012). Shrikhande et al. (2021) proposed DWC-MVR in algal biodiesel synthesis and conducted a sensitivity analysis for the effect of vapor split on the economic potential. However, a systematic optimization was not performed for the optimization of design and operational parameters. There are some studies addressing the MOO of biodiesel processes (Patle et al., 2014; Sharma and Rangaiah, 2013) considering the techno-economic objectives such as total annual cost (TAC) or profit. However, studies focusing on the optimization of algal biodiesel process considering eco-indicator (EI99) and individual risk (IR) as objectives are scarce. Recently, our study (Deshpande et al., 2022) implemented non-dominated sorting genetic algorithm (NSGA-II) for MOO of algal biodiesel process considering organic waste, CO_2 emission, TAC, and IR as the objectives. However, this process did not consider the application of DWC-MVR. Retrofitted processes are intricate and their optimization is required to verify the performance. Ani et al. (2021b) reported that MOO improves the performance of retrofitted processes in terms of operation, energy and environment. Tikadar et al. (2021b) worked on the MOO of the retrofitted process and reported the improvements in the economics of the process compared to existing counterpart. A number of tools are available for MOO of chemical processes. Ani et al. (2020) proposed the hybrid multiobjective differential evolution dynamic random local search (HMODE-DLS) algorithm. Authors observed that speed and quality of non-dominated solution was improved using HMODE-DLS. This algorithm is developed to improve the convergence of the Pareto optimal front and reported to be effective for the real-world complex problem (Ani et al., 2021a).

In this study, DWC-MVR retrofitted, ultrasound assisted and IL catalyzed in situ algal biodiesel process with triacetin (TAG) as a value-added product (obtained by acetylation of glycerol) is optimized using HMODE-DLS. HMODE-DLS is a recently developed excel based algorithm, very few investigators have used this algorithm for the MOO of any process. Therefore, evaluation of performance of this algorithm is also one of the uniqueness of this work. Among many important decision variables, overheat vapor split, liquid/vapor split from the distillation columns, and compressor duty are particularly critical. In the current study, three objective functions, namely break-even cost (BEC), EI99, and IR, are considered. This study is important as it covers economic, environmental, and safety aspect of this retrofitted process.

2. Process development

Ultrasound assisted transesterification by employing BBAIL catalyst for biodiesel production with a capacity of 20 kt/year from microalgae as a feedstock and TAG as a side product, is considered in this work. Ultrasound generates local pressure and temperatures (upto 1000 atm and 5000 K) and speeds up the reaction rate (Karmakar and Halder, 2019; Sawarkar, 2019). Non random two liquid (NRTL) thermodynamic model is employed for the calculation of activity coefficient and binary interaction parameter (Piemonte et al., 2016; Shrikhande et al., 2021). Validation of the thermodynamic model can be found in our earlier study (Shrikhande et al., 2021). It may be noted that the properties of BBAIL are not available in data base of the Aspen Plus. Therefore, structure of BBAIL is supplied and pertinent properties are provided in the software. Remaining properties are calculated using the UNIFAC group contribution method. Further, extractive-transesterification reaction kinetics is taken from Shrikhande et al. (2021). The process flowsheet for the biodiesel production from wet microalgae is shown in Fig. 1. The process design is based on the experimental outcomes and design reported earlier by our group (Shrikhande et al., 2021). Section 1 (experimentation and validation) in the supplementary information presents the summary of the experimental procedure and validation of results (See Table S2). The thermodynamic validation is presented in Figs. S4 and S5 in Section 2.1 of the supplementary information. *Scenedesmus sp.* microalgae is considered as feedstock with a composition of 82% water and 5% of lipid. *Scenedesmus sp.* contains various triglycerides, but all triglycerides are considered as triolein for convenience. Same assumptions were made by many authors (Sharma and Rangaiah, 2013; Piemonte et al., 2016; Patle et al., 2020). For 20 kt/year biodiesel production capacity, wet algae flow rate of 50332 kg/h is sent

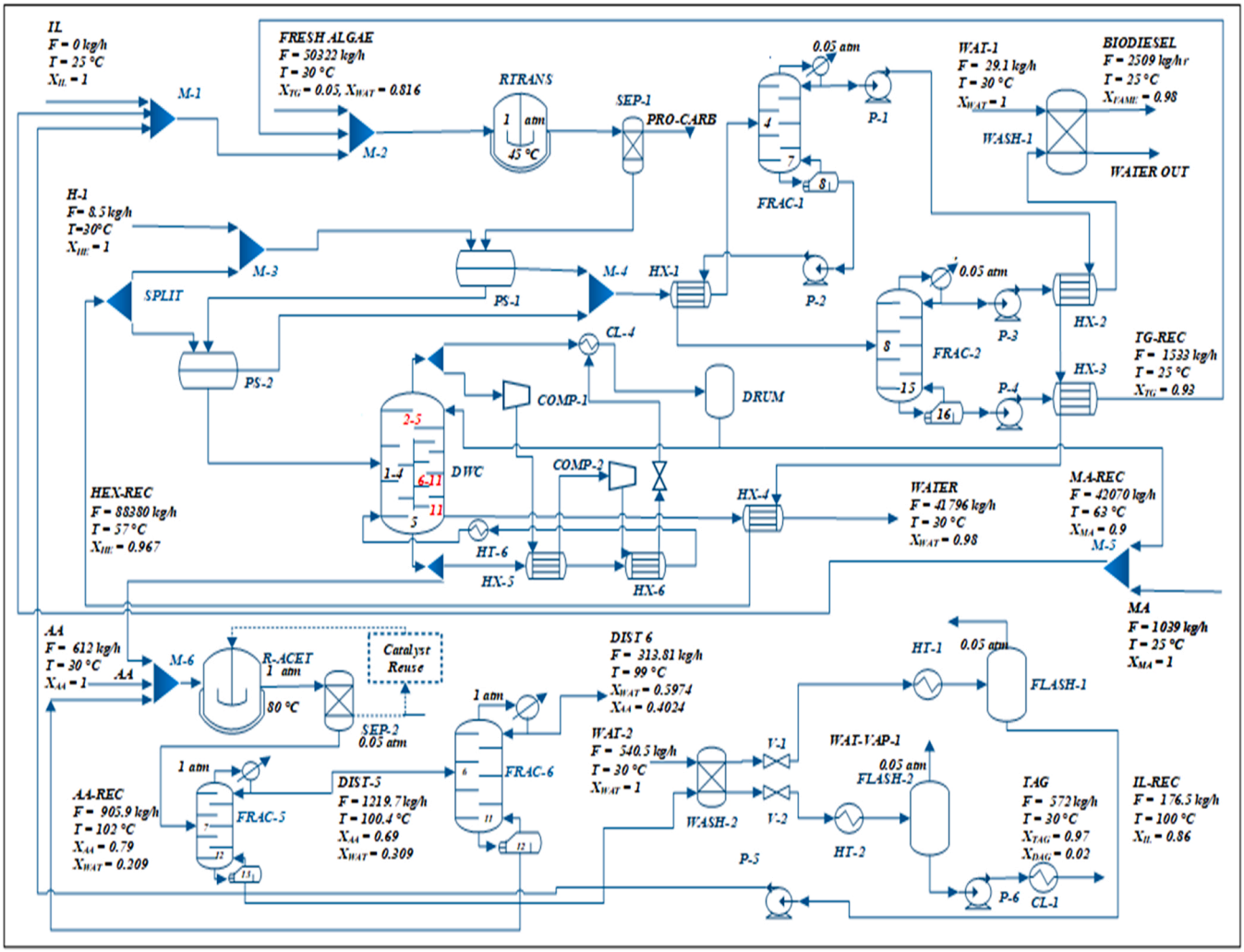

Fig. 1. Production of biodiesel from wet microalgae with DWC-MVR.

to the reactor RTRANS (RCSTR in Aspen Plus library).

RTRANS is designed for the residence time of 60 min and operates at a temperature of 45 °C and 1 atm pressure. BBAIL catalyst is supplied to the reactor at the flow rate of 200 kg/h. BBAIL catalyst gets recovered from the IL recycle and TG recycle stream (Fig. 1). Outlet of the rector contains protein, carbohydrate, biodiesel, BBAIL, unreacted methanol & lipids, and glycerol. Out of these, proteins and carbohydrates get removed in SEP1 (Simple component splitter in Aspen Plus library) and remaining components are sent to two phase separators, i.e. PS-1 and PS-2 (DECANTER in Aspen Plus library), where fresh hexane is supplied as a solvent. Organic phase contains hexane, biodiesel, and unreacted lipid. Lighter phase from the PS-1 and PS-2 are further sent to FRAC-1 (REDFRAC in Aspen Plus library). As biodiesel decomposes at ~250 °C, FRAC-1 operates under vacuum at 0.05 atm. Bottom stream from FRAC-1, comprising biodiesel and unreacted lipid, is sent to the FRAC-2 column. Distillate stream comprising hexane at − 12 °C is passed through the HX-2, HX-3, and HX-4 with the intention that the stream temperature reaches up to 40 °C, which is then reused in PS-1 and PS-2. Distillate from FRAC-2, containing 98% biodiesel at 238 °C, is then passed through the HX-2 to reduce its temperature to 25 °C. Bottom stream of the FRAC-2 containing lipid is recycled back to RTRANS reactor. FRAC-3 and FRAC-4, in our previous study (Deshpande et al., 2022), were used for the separation of water, methanol, and glycerol. Around 70% of steam consumption was attributed to FRAC-3 and FRAC-4. Composition and temperature profile of these two columns showed scope for combining them into the divided wall column (DWC) (Shrikhande et al., 2021). Heavier phase from the PS-2 enters in DWC on 3rd stage of left section of wall (i.e. FRAC-3). Vapors out of the reboiler are split just below the wall. Part of the vapor goes to the left section on 5th tray while the remaining goes to the 11th tray of the right section (FRAC-4). Similarly, liquid stream from the top section goes on 2nd tray of left side of wall and on 5th tray on right side of wall. Water is withdrawn from the right side of the column from 11th tray. The vapors from the DWC column are compressed in compressor to increase the temperature of the vapor stream. This rise in temperature is utilised in the reboiler of the DWC. As bottom and top temperature difference of the DWC is high, suggesting the wide boiling mixture, single stage compressor turns out to be uneconomical. Also, energy produced by the single compressor is insufficient to provide the heat required in the reboiler. Hence, MVR methodology is adopted in this retrofitted process. Distillate vapors from the DWC are split into two streams out of which one goes to condenser CL-4 and other goes to compressor. COMP-1 operates at compression ratio of 3.5. Heat of the compressed vapor stream from COMP-1 is transferred to HX-5 which acts a reboiler of DWC. Vapor stream from HX-5 is then further compressed in COMP-2. Again, hot vapor stream after COMP-2 is passed through HX-6, which also acts as a reboiler of DWC, similar to HX-5. Vapor from the HX-6, condensed after transferring heat, are then returned to condenser through throttling valve to make the vapor stream pressure equal to condenser pressure i.e., 1 atm. All vapor gets condensed in condenser CL-4 and total liquid is then sent to reflux drum (DRUM). From reflux drum, one stream enters back into DWC as reflux and other stream

containing mainly methanol (96.0%) is recycled back to the RTRANS. Bottom stream from the DWC is passed through HX-5 and HX-6 as reboiler. The bottom stream is split into two: one goes back to DWC and other stream containing mainly glycerol is used in further downstream process.

Bottom product from the DWC, mainly containing glycerol, is further reacted with acetic acid in ratio of 8:1 R-ACET (RSTOIC in library of Aspen Plus) that operate at 1 atm and 80 °C (Deshpande et al., 2022). R-ACET outlet containing TAG, monoacetin (MAG), diacetin (DAG), BBAIL and unreacted acetic acid is then supplied to FRAC-5 (RADFRAC in library of Aspen Plus) on 6th stage. In FRAC-5, azeotrope of the water and acetic acid is obtained as a distillate, whereas TAG, MAG, DAG, and BBAIL are obtained as bottom product. Distillate of the FRAC-5 is sent to FRAC-6 for further recovery of the acetic acid. Nearly 80% of the acetic acid is recovered from the bottom of the FRAC-6, which is recycled back to the R-ACET. Bottom product from the FRAC-5 is then sent to WASH-2 (EXTRACT in Aspen Plus library). BBAIL and water are further supplied to the FLASH-1 through heater 'HT-1'. In FLASH − 1, water vapor is removed from top and BBAIL catalyst is recovered and recycled back to the RTRANS reactor. TAG, water and small amount of DAG and MAG are sent to FLASH-2 through HT-2 to obtain 97% pure TAG.

3. Multiobjective optimization framework

The goal of sustainable design is to reduce environmental, economic, and social implications early in the design process (Sánchez-Ramírez et al., 2017). MOO is the methodology of systematically and concurrently optimizing all objective functions, which are often conflicting in nature, to find the solution that is the best compromise of all (Marler and Arora, 2010). Optimization has become necessary for chemical process industry, particularly in light of environmental and safety regulations (Thafseer et al., 2021; Tikadar et al., 2021b). Ani et al. (2020) proposed the hybridisation of the multiobjective differential evolutionary (MODE) algorithm by adding one of the simple local search methods to speed up the convergence of the Pareto optimal front and quality of non-dominated solutions. A random dynamic local search approach is used for the hybridisation of MODE, referred to it as HMODE-DLS. MODE algorithm searches the global space and the hybridised dynamic local search (DLS) searches the nearby neighbourhood area of higher fit population. HMODE-DLS aids in directing and guiding the integrated algorithm for improving the convergence of Pareto optimal front. Created solutions will have two sources in each of the generation, i.e., DLS and MODE. In HMODE-DLS, the population size (Q) is divided into two parts- one-part aQ is from conventional MODE and bQ is from the dynamic local search to generate new population, where a+ b = 1. Ani et al. (2020) compared the performance of HMODE-DLS and MODE. Authors reported that HMODE -DLS converges much earlier than the MODE algorithm. This is due to the participation of DLS in the decision space searching operation with MODE algorithm. Authors reported that HMODE-DLS outperformed the MODE on the ground of convergence, spread, generational distance and spacing, and found that results obtained are more accurate and faster.

This optimization study aims at minimization of breakeven cost (BEC), impact of the process on environment (EI99), and individual risk of plant (IR) of proposed in situ ultrasound assisted DWC-MVR retrofitted biodiesel process.

$$Minimize \quad (BEC, \quad IR, \quad EI99) \quad = \quad f \quad (Decision \quad variable)$$

$$Subject \quad to \quad constraint: \quad x_L \quad \leq \quad constrain \quad \leq \quad x_U$$

x_L = lower boundary of decision variable and x_U = upper boundary of decision variable $g(x) \leq 0$

$$h(x) \quad = \quad 0 \tag{1}$$

Where, BEC, EI99, and IR are the objectives or targets to be minimized, x is a vector of decision variables, which can take any value between practical values selected as lower and upper limits of x_L and x_U, respectively, and g(x) and h(x) are inequality and equality constraints, respectively. Table 1 presents the objective functions and constraints considered in the present investigation. Temperature and residence time of the reactor influences the lipid conversion into biodiesel. Feed plate of the distillation column affect the steam consumption of the reboiler.

As this process is retrofitted with DWC-MVR, vapor split into each side of the wall in DWC (VAP-SPLIT-F3) and liquid split on each side of the wall in DWC (LIQ-SPLIT-F4) are crucial for decreasing the reboiler and condenser duties. In MVR, overhead vapor split (OH-VAP-SPLIT) is prominent as it dictates the compressor load and energy efficiency.

Similarly, compression ratio of compressor 2 (COMP2-CR) is important as it dictates the energy rise in the vapor stream at the cost of electricity consumption. Therefore, all above variables are considered as decision variables. Biodiesel produced from the process must meet the required standards. Hence, purity of biodiesel (0.965), triacetin (0.96), recycled methanol (0.88), recycled hexane (0.95) are kept as constraints. In order to prevent the degradation of biodiesel and triacetin, bottom temperature of distillation column is also taken as constraint. Compressor 2 increases the temperature of the vapor stream and its outlet temperature is taken as constraint for the safety.

In this MOO study, Excel based HMODE-DLS program is linked with Aspen Plus by employing visual basic application. Fig. 2(a) presents the HMODE-DLS algorithm and Fig. 2(b) presents the integrated framework for the MOO of biodiesel process. This framework can be extended to any process that can be simulated in the flowsheeting softwares. HMODE-DLS suggests the set of decision variables, which is supplied to Aspen Plus. Further, simulation is run and required parameters are supplied to excel for further calculation of decision variables. Objective functions are subsequently calculated. Satisfactory results are then sorted using the HMODE-DLS algorithm. HMODE-DLS parameters used in the present investigation are: Population size = 100, Crossover probability = 0.75, Mutation factor = 0.3, Local scaling factor = 0.5, and maximum number of generations = 100.

3.1. Break even cost (BEC)

To evaluate the economic performance of the process, breakeven (BEC) cost is considered as an objective. BEC is the cost at which a company's revenue equals its cost of manufacturing. Thus, the cost of manufacturing (COM) is equal to the revenue generated by selling the products (including the by-product). BEC of the process is calculated by equating the COM (Eq. (3)) that includes capital cost, raw material cost, utility cost, and labour cost (Turton et al., 2008). BBAIL catalyst from the reactor goes to FRAC 1 and FRAC 2 through the phase separators, and is recycled back to the reactor through TG-REC stream (Fig. 1). Similarly, BBAIL catalyst which goes to DWC-MVR from the heavy phase from phase separators is recycled back to the reactor through IL-REC stream

Table 1
Different optimization cases studied for production of algal biodiesel.

Objective function	Decision variables	Constraints
Case A:	$35 \leq T_{TRANS} \leq 60$ °C	Mass purity: $x_{Biodiesel} \geq 0.965$
min. BEC	$55 \leq$ (Residence Time) $_{RTRANS} \leq 85$ min	Mass purity: $x_{Glycerol} \geq 0.96$
($/kg)		(Methanol-Hexane Recovery) $_{FRAC-4} \geq 0.88$
min. EI99	$2 \leq$ (Feed Stage) $_{FRAC-1} \leq 7$	
Case B:	$2 \leq$ (Feed Stage) $_{FRAC-2} \leq 15$	(Hexane Recovery) $_{FRAC-1} \geq 0.95$
min. BEC	$2 \leq$ (Feed Stage) $_{FRAC-3} \leq 5$	
($/kg)	$2 \leq$ (Feed Stage) $_{FRAC-5} \leq 12$	$T_{FRAC-1} \leq 250$ °C
min. IR	$2 \leq$ (Feed Stage) $_{FRAC-6} \leq 11$	$T_{FRAC-2} \leq 290$ °C
Case C:	$290 \leq$ (VAP-SPLIT-F3) ≤ 440	$T_{FRAC-5} \leq 150$ °C
min. BEC	$2000 \leq$ (LIQ-SPLIT-F4) ≤ 2900	$T_{FRAC-6} \leq 150$ °C
($/kg)		$T_{COMP2\_OUT} \leq 300$ °C
min. EI99	$2.2 \leq$ (COMP2-CR) ≤ 4.2	
min. IR	$0.4 \leq$ (OH-VAP-SPLIT) ≤ 0.8	

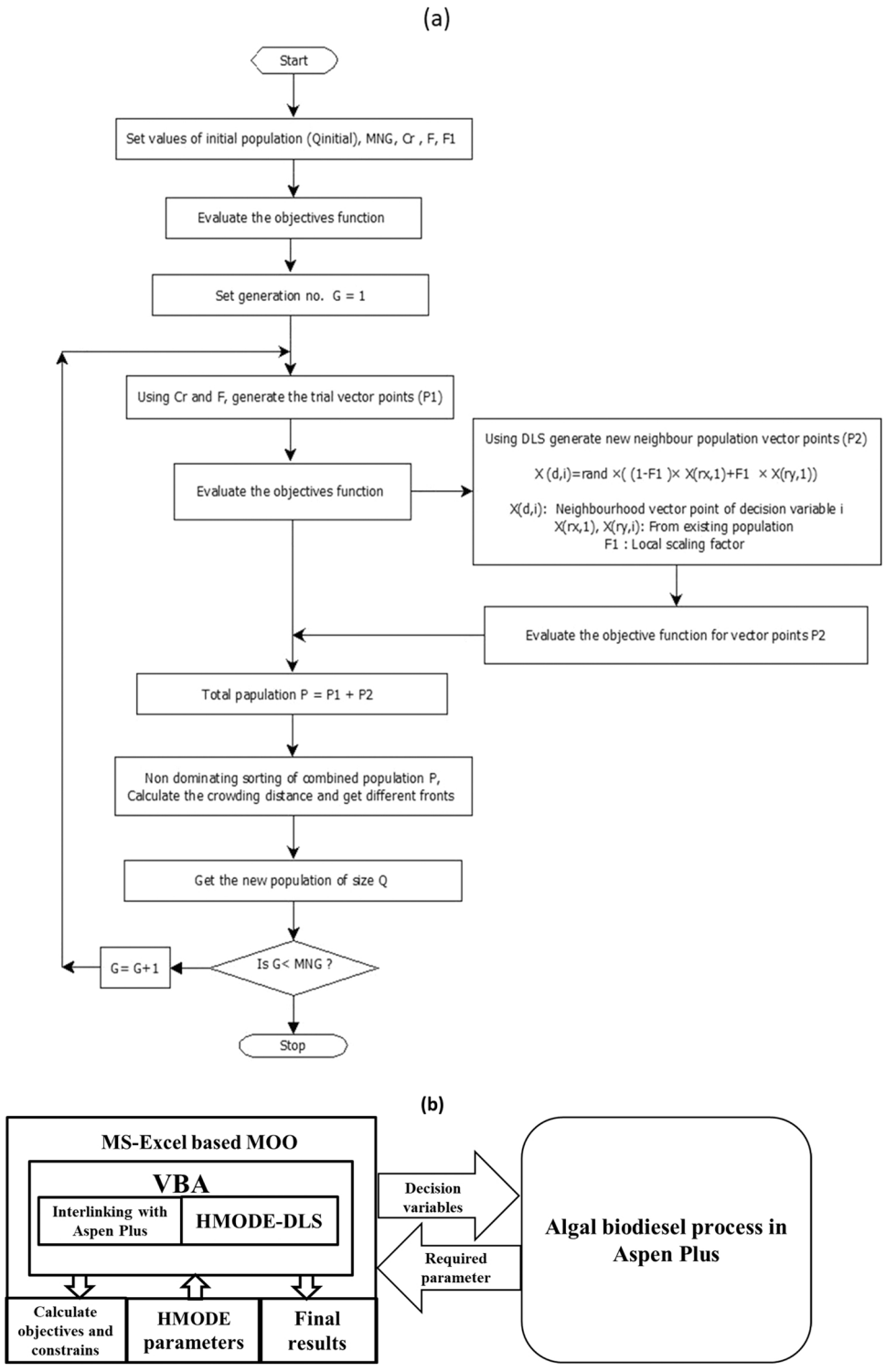

Fig. 2. (a) HMODE-DLS algorithm [MNG: Maximum number of generations, Cr: Crossover frequency, F: Mutation factor, F1: Local scaling factor (DLS)] Ani et al. (2020); (b) Integrated framework depicting MOO of retrofitted algal biodiesel production process.

(Fig. 1). Therefore, theoretically complete BBAIL catalyst is recycled back to process and it is assumed that the cost of BBAIL is not too significant in the long run though it is expensive. Hence, reuse of BBAIL catalyst has been accounted in COM calculation. Section 2.2 in the supplementary information presents the design parameters, costs of equipments, and cost of utilities. All equipment sizes and the costs are determined by the procedure given by Turton et al. (2008). D/L ratio of 1:2 is maintained for all the process equipments which is desired for good control (Luyben, 2002). Volume of the reactors and phase separators are calculated from the required residence times. For estimating the cost of distillation column, diameter is taken from the Aspen Plus and height of the column is estimated from number of stages. Tray spacing is taken as 0.6 m, whereas free space of 20% (at the top and the bottom) of calculated height (number of trays × tray spacing) is assumed. Reboiler and condenser are considered as separate stages. Number of trays in column is determined by performing sensitivity

analysis with the objective of reducing the TAC of column.

While in costing the DWC-MVR, DWC is segregated into three sections. Top section contains stages 1–5 (FRAC-4), whereas in the middle section, left side of the DWC represents FRAC-3 and right side of the wall represents FRAC-4 of process from our previous study (Deshpande et al., 2022). The bottom section of the DWC contains a single tray of FRAC-3. Total height of the column is the sum of top, middle, and bottom section of the column. 20% of total height is added for the top and bottom spacing of the column. From the volume of the column, cost is estimated as per procedure (Turton et al., 2008). A 50% penalty is imposed to the column's computed cost, which includes wall and other accessories costs (Xu et al., 2017). The cost of the heat exchanger, used as reboiler in DWC-MVR, and condenser are calculated from the heat duty obtained from Aspen Plus using the guideline given in Turton et al. (2008). Cost of the compressors is estimated from the CAPCOST MS excel program that is based on the correlations given in Turton et al. (2008). Finally, cost of the DWC is evaluated by the summation of all above costs.

Chemical engineering plant cost index (CEPCI) of 607.5, which considers of inflation in 2019, is taken in this work. Bare module cost (BMC) is calculated by multiplying the bare module factor with the purchase cost of each equipment. Then, Total module cost (TMC) is calculated by Eq. (2) (Turton et al., 2008). Utility cost for heater, cooler, reboiler and condenser is calculated from the heat duty obtained from the Aspen Plus. For calculating electricity requirement of pumps and compressors, shaft power has been taken from Aspen Plus.

$$TMC = 1.18 \quad BMC \tag{2}$$

Cost of manufacturing (COM) is calculated as per Eq. (3) given in Turton et al. (2008).

$$COM = 0.28TMC + 2.73(labor \quad cost) + 1.23(utility \quad cost + raw \quad materials \quad cost) \tag{3}$$

The operating cost includes the raw materials' cost such as cost of microalgae, hexane, methanol, and BBAIL catalyst. Utilities cost includes the cost of cooling water, refrigerant, steam, and electricity. Operating labor cost is calculated as per the procedure given in Turton et al. (2008). Unit raw material cost and utility cost are taken from Shrikhande et al. (2021). The plant is assumed to operate for 8000 h in a year for the calculation of BEC. Supporting equations with references and sample calculation for the estimation of BEC of the process is given in Section 3 of supplementary information.

3.2. Eco indicator 99 (EI99)

The Eco-Indicator 99, which is based on the life cycle assessment, is used to assess the process' long-term viability and quantify the environmental impact of the various activities included in the process (Contreras-Zarazúa et al., 2021; Goedkoop and Spriensma, 2001). When assessing the environmental implications of chemical processes and biorefineries, this methodology has reported to be efficient (Contreras-Zarazúa et al., 2019). By measuring and quantifying the material and energy utilized, the EI99 allows for the evaluation of the environmental burden associated with a specific process or a product. One point on the EI99 scale represents a 1000^{th} part of an average European citizen's annual environmental burden (Ramírez-Márquez et al., 2019).

It is reported that using the Eco indicator 'EI99' during the design and synthesis phases, can result in significant improvements and waste reductions (Contreras-Zarazúa et al., 2021). The approach used to calculate EI99 considers 11 different impact categories. According to the type of the damage, the 11 categories are divided into three groups: (i) human health, (ii) ecosystem degradation, and (iii) natural resource damage. Three impact elements are evaluated in this study while calculating EI99: steam for heating, electricity for pumps and compressor, and steel utilized in the construction of main equipments. Hence, steam, steel, and electricity used by the process is multiplied by the pertinent impact factor from the Table 2 and weighting factor. Damage weighting factor to human health and ecological quality are both considered as equally significant, however, damage to resources is considered as just approximately half as important (Martinez-Gomez et al., 2016). Additionally, the hierarchical perspective was considered in the provided approach to balance the short- and long-term consequences. The damage computation for all relevant extractions, emissions, and land-use is used to create the normalising set (Contreras-Zarazúa et al., 2019).

$$EI99 \quad = \quad \sum_{b}\sum_{d}\sum_{k\in K}\delta_d \quad \omega_d\beta_b \quad \alpha_{b,k} \tag{4}$$

Where, δ_d: normalisation factor for damage in category d, ω_d: damage weighting factor for category d, β_b: amount of chemical b released by direct emission per unit of reference, and $\alpha_{b,k}$: damage in category k per unit of chemical b released to the environment. As the algal feed to the reactor is kept constant, there will not be any change in size /weight of the plant, hence, weight of the plant is considered constant. Sample calculations for the estimation of EI-99 is provided in Section 3.2 of supplementary information.

3.3. Individual risk

Process safety is the main concern in chemical industry. The number of accidents involving hazards is increasing every day, resulting in plant shutdown, environmental hazards and human injury (Tikadar et al., 2021a). The process safety of the process is measured using the individual risk (IR) index. IR is the probability of a person dying as a result of a loss of containment incident (Medina-Herrera et al., 2014). IR is calculated by multiplying the frequency of the accident (fi) by the probability of affectation in a particular position (Px,y).

$$IR \quad = \sum_{0}^{i} f_i P_{xy} \tag{5}$$

where, fi is the frequency of occurrence of incident i, and Px,y is the probability of injury or death produced by the incidence occur i (AIChE, 2000). Quantitative risk analysis (QRA) is used to calculate the frequency and probability of occurrence. The QRA technique allows for the detection of probable accidents as well as the assessment of their repercussions and damages (Haag, de, Ale, 2005). There are two types of potential incidents: continuous releases, which involves the leakage of matter from process equipment owing to a pipeline rupture, and instantaneous releases, which involves the whole loss of matter from process equipment due to a catastrophic vessel rupture (Contreras-Zarazúa et al., 2019; Medina-Herrera et al., 2014).

Potential incidence occurrences are discovered by HAZOP. The possible event and their frequencies are given in AIChE (2000). Boiling

Table 2
Unit Eco-indicator used to measure the Eco-indicator 99 (Goedkoop and Spriensma, 2001).

Impact category	Steel (points/kg)	Steam (points/kg)	Electricity (points/kWh)
Carcinogenic	6.32×10^{-03}	1.18×10^{-04}	4.36×10^{-04}
Climate change	1.31×10^{-02}	1.60×10^{-03}	3.61×10^{-06}
Ionizing radiation	4.51×10^{-04}	$1.13\times10^{+00}$	8.24×10^{-04}
Ozone depletion	4.55×10^{-06}	2.10×10^{-06}	1.21×10^{-04}
Respiratory effects	8.01×10^{-02}	7.87×10^{-07}	1.35×10^{-06}
Acidification	2.70×10^{-03}	1.21×10^{-02}	2.81×10^{-04}
Ecotoxicity	7.45×10^{-02}	2.80×10^{-03}	1.67×10^{-04}
Land occupation	3.73×10^{-03}	8.58×10^{-05}	4.68×10^{-04}
Fossil fuels	5.93×10^{-02}	1.25×10^{-02}	1.20×10^{-03}
Mineral extraction	7.42×10^{-02}	8.82×10^{-06}	5.70×10^{-06}

liquid expanding vapor explosion (BLEVE), Unconfined vapor cloud explosion (UVCE), flash fire and toxic release are the accidents that come under the instantaneous release, identified by HAZOP analysis. Whereas, jet fire, flash fire and toxic release are the accidents that can occur in case of continuous release. When incidents are detected, the probability Px,y can be estimated using a consequence evaluation, which involves identifying thermochemical variables such as thermal radiation, over-pressurization, and the concentration of the leak caused by the incidents, and their respective damage(AIChE, 2000; Contreras-Zarazúa et al., 2021). For the case of flash fire and toxic release, the dispersion is considered using the atmospheric stability type F, which corresponds to a wind speed of 1.5 m/s which is the worst-case situation (AIChE, 2000; Crowl and Louvar, 2002). There is no equation that represents the behaviour and thermal radiation produced during the event due to the short duration of the flash fire. As a result, first flammable material's concentration is determined by using Pasquill-Gifford Model (Crowl and Louvar, 2002) and if the concentration is in between the lower flammable limits (LFL) and upper flammability limit (UFL), then it is assumed that the thermal radiation produced by a flash fire is sufficient to pose a hazard. In the incidence of toxic release, the concentration determined using the Pasquill–Gifford Model is compared to the LC_{50} (median fatal concentration) to see if it is more than what an organism can tolerate (Contreras-Zarazúa et al., 2019). LFL, UFL and LC_{50} values are taken from Deshpande et al. (2022). Supporting equations and sample calculation for the estimation of IR of the process is given in Section 3.3 of supplementary information.

After identifying all probable accidents, the next step is to calculate the probit function (Y) for each outcome. Eq. (6) provides the relationship between probit function in view of the thermal radiation and overpressure due to explosions (p) with the probit variable (Y). The values of k1 and k2 (constants for the respective event) stated by Crowl and Louvar (2002) are given in Table 3. Calculations are based on a distance of 100 m. Eq. (7) is used to compute the probability of affectation (Px,y) from the causative factors of the relevant end result and the probit function (Haag, de, Ale, 2005).

$$Y = k1 + k2 \; lnV \tag{6}$$

$$P = 0.5 \left[1 + erf\left(\frac{|Y - 5|}{\sqrt{2}}\right)\right] \tag{7}$$

4. Results and discussion

In this section, results of optimization of retrofitted algal biodiesel process using HMODE-DLS algorithm are discussed. The optimization study is carried out by changing the decision variable presented in the Table 1. First, two bi-objective optimization cases, namely BEC vs EI99 (Case A) and BEC vs IR (Case B) are studied. Subsequently, all three objectives (i.e., BEC, IR and EI99) are simultaneously optimized. At last, best solution from the obtained Pareto optimal front is estimated using the simple additive weight (SAW) method.

4.1. MOO of BEC and EI99 (Case A)

Fig. 3 represents the Pareto optimal front for the simultaneous optimization of BEC and EI99. Each point on the graph represents the separate design for the process for minimized BEC and EI99. BEC is based on the COM, which is a function of capital investment, raw material cost, utility cost and labour cost. Hence, the minimum BEC means the minimum COM. EI99 depends on the steam, electricity, and steel usage. As algal feed to reactor is kept constant to get continuous production of biodiesel at a constant rate, design parameters (size) of the equipments largely remain constant. Hence, amount of the steel usage in the EI99 calculation does not change significantly. Fig. 3(a) clearly indicates the conflict between BEC and EI99. Decrease in BEC is complimented by the increase in EI99. It is important to understand that the utility (electricity and steam) consumption contribute to both objectives in a similar way. Nevertheless, the trade-off between the objectives is a result of the effect of decision variables on the product formation and utility consumption. EI99 was found to decrease from 21.1×10^5 to 10.81×10^5 at the cost of increase in BEC from \$1.85 to \$5.08 per kg. From Fig. 3(b), optimum temperature of the reactor (RTRANS) is scattered majorly near to the lower bound. Reactor temperature influences the conversion of lipid into biodiesel. Hence, the rise in the reactor temperature increases the BEC of the biodiesel, whereas it increases the EI99 because of the increase in steam consumption. Variation of optimal residence time of reactor with BEC is shown in Fig. 3(c). Higher is the residence time, the greater is the conversion that results in the decreased BEC. But the higher residence time means the larger reactor size and greater consumption of the utility, resulting in the increased EI99. Consequently, optimal residence time lies in the middle of the lower and upper bounds (65–75 min). Optimum feed plate can reduce the utility consumption in the distillation columns as it results in reduced reboiler duty. Fig. 3(d)-(h) show the optimal feed plate for the distillation columns. Largely, the optimum feed plate for each distillation column lies in the middle of the upper and lower bounds, except for FRAC-3 that separates glycerol and methanol-water. Optimum feed plate contributes to the reduced utility consumption, thereby resulting in the reduced BEC as well as EI99. As this process is retrofitted with DVD-MVR, LIQ-SPLIT-F4, VAP-SPLIT-F3, COMP2-CR, and OH-VAP-SPLIT (Table 1), are crucial decision variables as they denote the success of the retrofitting.

From Fig. 3**(i-j)**, it can be seen that all optimal points for LIQ-SPLIT-F4 and VAP-SPLIT-F3 lie in the lower half of the plot, i.e., below the respective base case value of 366 kmol/h and 2460 kmol/h. Optimal LIQ-SPLIT-F4 contributes to the optimal operation of the DWC by optimally splitting the liquid coming from the top section of DWC on the either side of the wall, resulting in the reduced reboiler duty. Similarly, optimal VAP-SPLIT-F3 results in the minimization of the objectives by optimally dividing the vapors generated in the reboiler on the either side of the wall of DWC. The optimal points for COMP2-CR (Fig. 3**k**) are largely scattered in middle of the plot (between 3.25 and 3.75) against the base case value 3.5. As COMP2-CR increases, capital and operating cost (electricity consumption) of the process increases. This results in increase in BEC and EI99. Therefore, optimal compression ratio is important as it results in the reduced steam consumption in the reboiler duty, which contributes to the minimization of BEC and EI99. Similarly, OH-VAP-SPLIT (Fig. 3**i**) is scattered in lower half of the plot, i.e. between the 0.4 and 0.6. Optimum OH-VAP-SPLIT is essential as the amount of vapors entering the compressor decides the capital and operating cost of the compression. On the one hand, the smaller amount proves to be insufficient for imparting the enough energy in HX-5 and HX-6 (representing the reboiler of DWC), whereas greater amount of vapor entering into the compressor results in increased capital and operating cost.

4.2. MOO of BEC and IR (Case B)

Pareto optimal front for the simultaneous minimization of BEC and IR is presented in Fig. 4(a). A clear trade-off between these two objectives is evident from Fig. 4(a). Higher the quantity of material, higher is the risk involved in the process. IR depends on the explosive and toxic properties of the material. Explosions depend on heat of combustion of the materials. For toxicity, LC_{50} is considered as limiting concentration. UFL and LFL are considered for the estimation of flash fire. Presence of water in released material decreases the risk as some toxic materials may be soluble in water and get diluted to a lower concentration of explosive

Table 3
Probit model parameters.

Incident	K1	K2	V
BLEVE, JET FIRE	-14.9	2.56	Thermal radiation
UVCE	-77.1	6.91	Overpressure

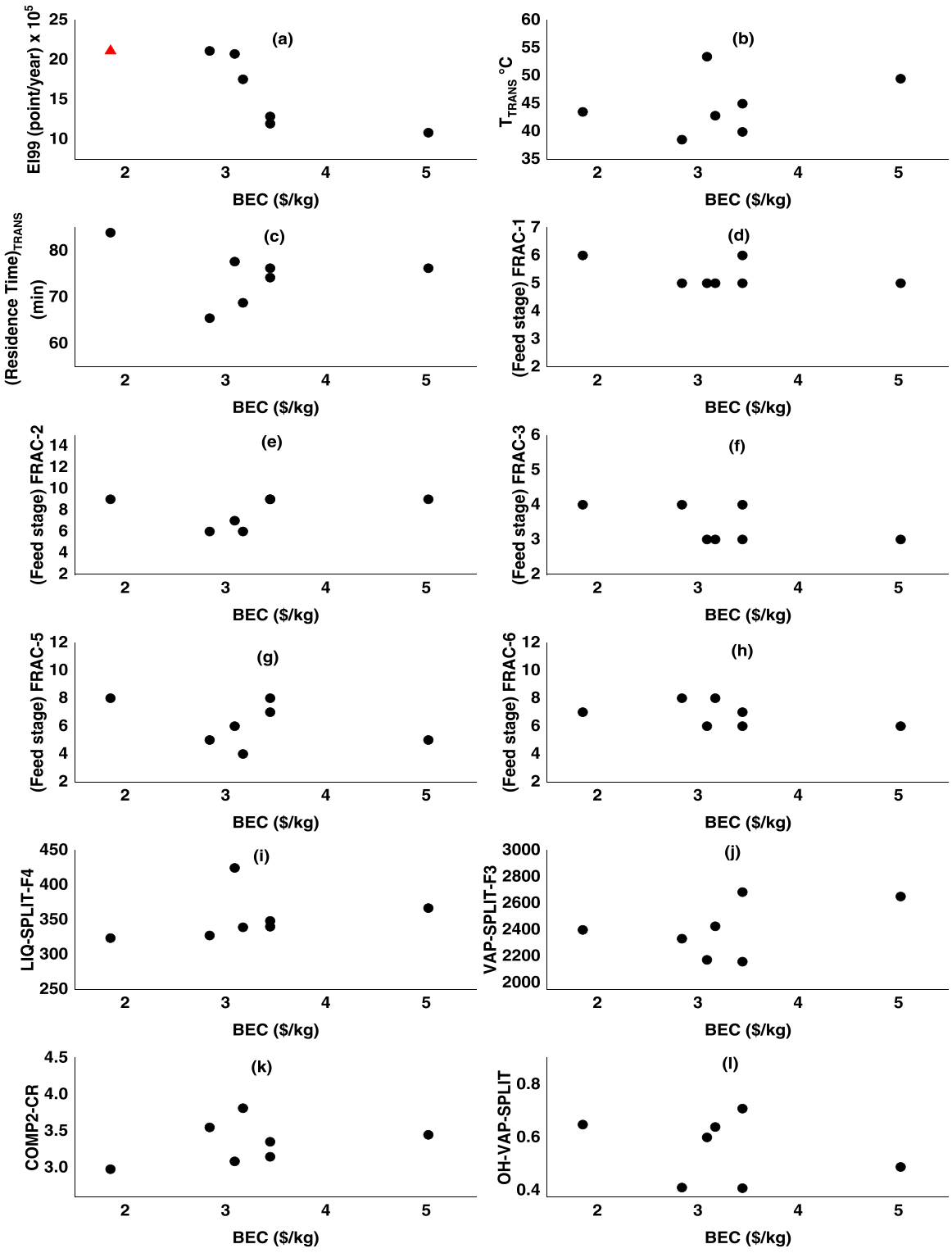

Fig. 3. Simultaneous optimization of BEC and EI99.

material, thereby resulting in lowering the intensity of the accidents. Pareto optimal front between the two objectives is antagonist in nature. The decrease in the IR from 2.01×10^{-5} to 1.26×10^{-5} per year is accompanied by the increase in BEC from \$2.19 to \$4.12 per kg. IR depends on residence time in the reactors and phase separators, reflux ratio of the distillation columns, and internal flow through MVR of DWC-MVR. On the other hand, BEC of the process depends on the capital cost and operating cost. Fig. 4(b) shows the optimum temperature for the minimization of BEC and IR. Optimum temperature of RTRANS (Fig. 4b) are largely scattered between the upper and lower bounds. It is due to the fact that the lower temperature increases the BEC (due to the decrease in the conversion of lipid into biodiesel), and it decreases the IR as the biodiesel is more hazardous than the unconverted lipid. From Fig. 4(c), the optimum residence time of reactor is found to be in the upper half of the plot (between 65 and 75 min). Greater the residence time in the reactor, greater the lipid conversion into the biodiesel (which

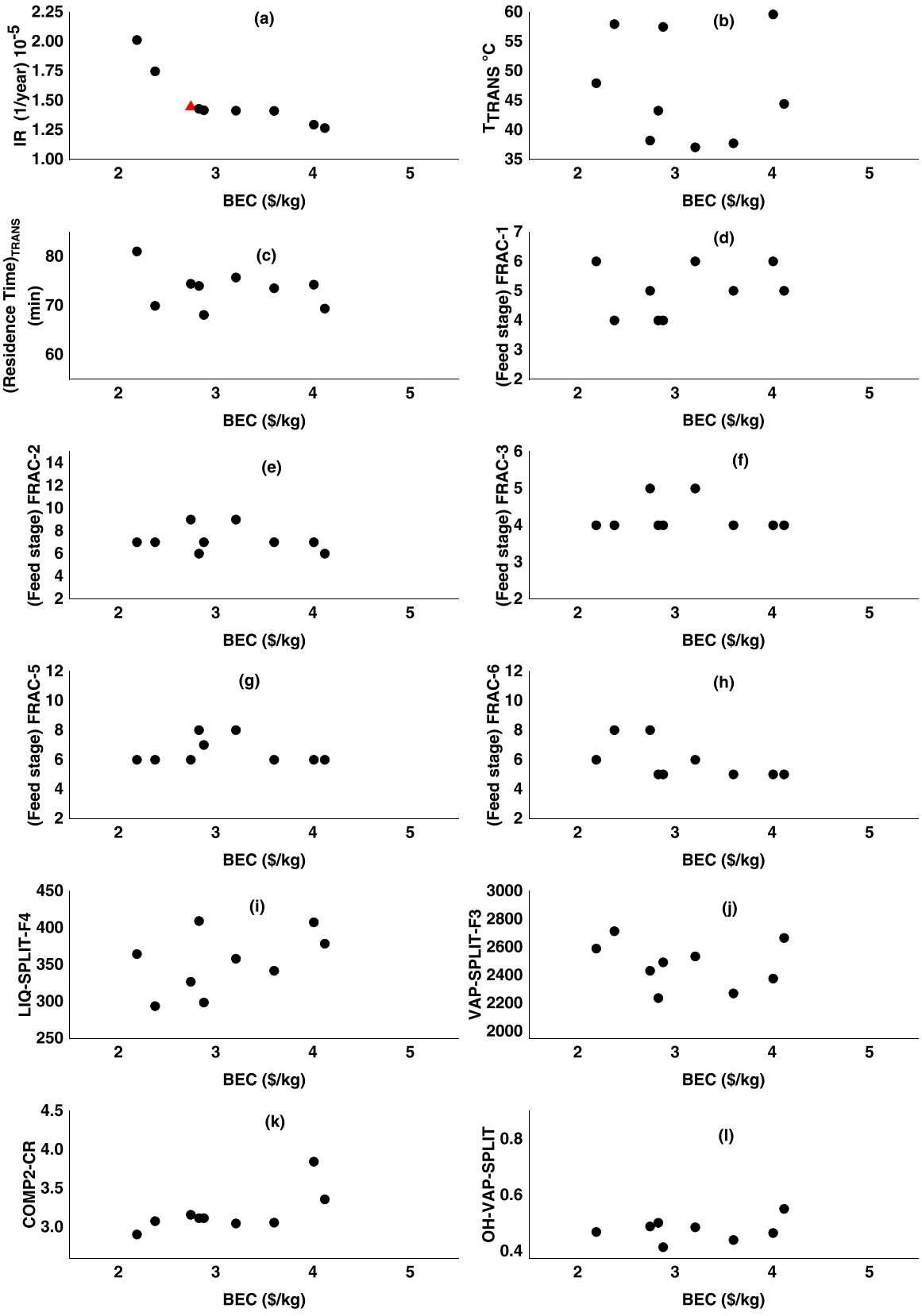

Fig. 4. Simultaneous optimization of BEC and IR.

favors the BEC positively). However, greater residence time depicts the increased capital cost which affects the BEC negatively. In addition, increase in the residence time increases the material inside the reactor, thereby it causes the increase of the IR. Fig. 4(d-h) show the optimal feed plate for the distillation columns. For FRAC-1 and FRAC-3 (left side of DWC), the feed plate location is scattered in the upper half of the plot. For remaining columns, the optimal feed plates lie in middle of the upper and lower bounds. It may be noted that the feed tray location can influence the size as well as the utility consumption of the distillation systems. Maximum reflux depicts the increased internal flow, which results into increased IR for the process. Optimal LIQ-SPLIT-F4 (between 300 and 400 kmol/h) and VAP-SPLIT-F3 (between 2200 and 2600 kmol/

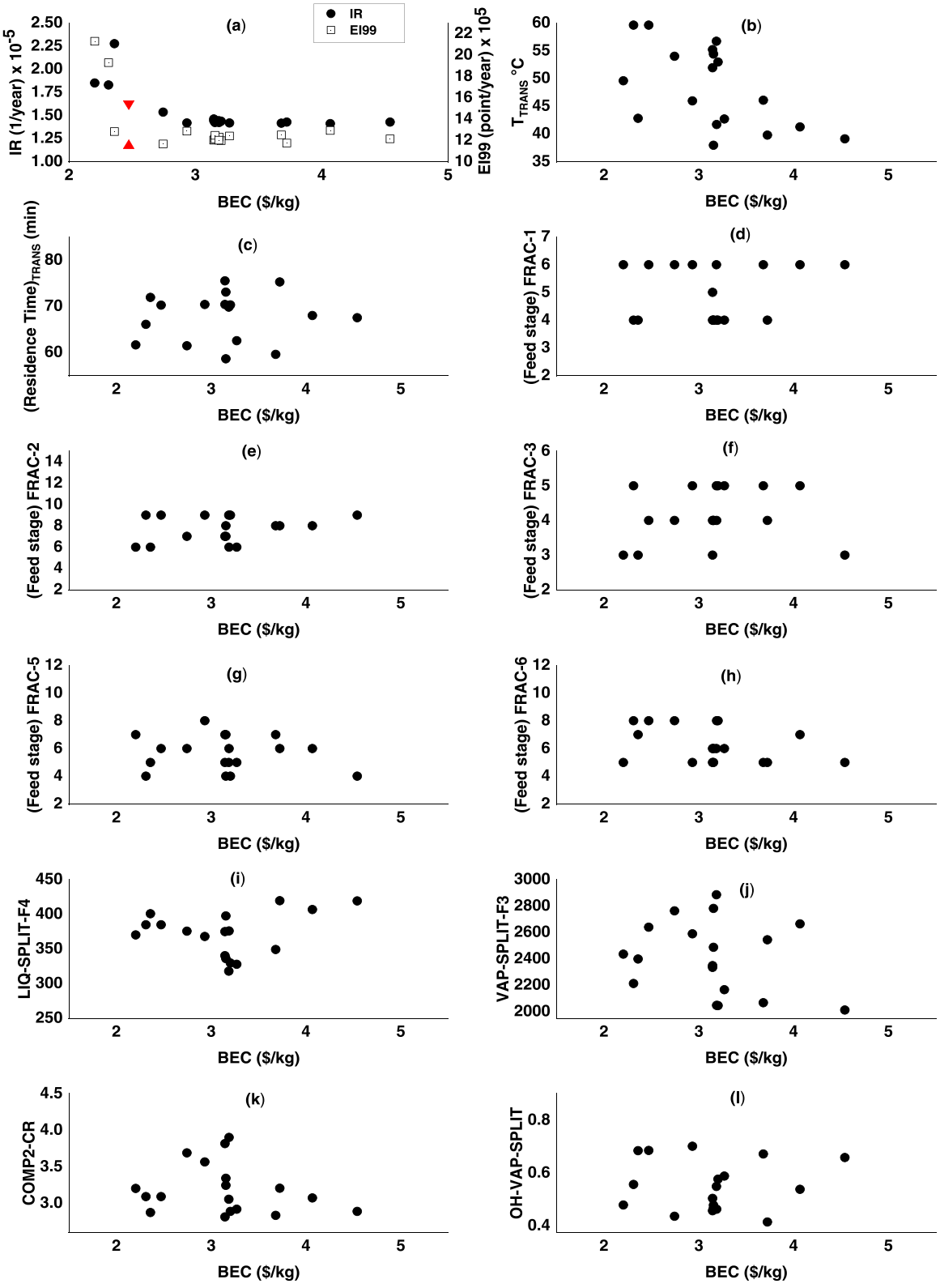

Fig. 5. Simultaneous optimization of BEC, EI99, and IR.

h) are settled in middle of the plots, as they can be seen in Fig. 4(i) and Fig. 4(j), respectively. These optimal points ensure the reduced reboiler duty of DWC, resulting in the decreased BEC. Here, it is noteworthy to understand that sufficient split of the liquid and vapor is required on each side of the wall of DWC to ensure its proper operation. At the same time, optimal COMP2-CR and OH-VAP-SPLIT, whose original value are 3.5 and 0.45 respectively (Fig. 1), are required to minimize BEC and IR. From Fig. 4(k) and Fig. 4(l), it can be observed that the optimal points lie near to the lower bounds. As COMP2-CR increases, the capital and operating costs (in term of electricity consumption) also increase, resulting in the increased BEC. Similarly, as the OH-VAP-SPLIT increases, the load on the compressor also increases, causing the increase in the BEC of the process. Increased COMP2-CR and OH-VAP-SPLIT result in the increased IR for these equipments.

4.3. MOO of BEC, EI99 and IR (Case C)

In cases A and B, only bi-objective optimization studies are conducted to understand the trade-offs between BEC and other objectives (i.e. EI99 and IR, individually). Further in case C, all three objectives are simultaneously minimized to understand the overall scenario. Fig. 5(a) shows the trade-off between BEC and EI99 and BEC and IR for the simultaneous optimization of all three objectives. In Fig. 5(a), square points represent the trade-off between BEC and EI99, whereas the dotted points represent IR. The point marked as 'Δ' denotes the points obtained from simple additive method (SAW), explained in the next section. Fig. 5 (a) clearly shows that the trade-offs between BEC and EI99 and BEC and IR are qualitatively similar to those obtained in Case A and Case B, respectively. From Fig. 5(a), it can be seen that EI99 and IR are conflicting with the BEC of the process. EI99 and IR of the process decrease at the cost of increase in BEC of the process. IR, which is a critical indicator for the evaluation of the safety of the process, is reduced by 38%. EI99, which is related to the environmental burden from the plant, is reduced by 46%.

It is observed that temperature of the reactor is largely scattered between the upper and lower bounds (Fig. 5b). Temperature of the reactor affects all three objectives simultaneously. As the temperature of the reactor increases, conversion of lipid also increases. This causes the increase of the IR, while favouring the BEC. Increase in temperature of the reactor also increases the EI99 because of the increased steam consumption. Optimal residence time of reactor (Fig. 5c) lie in the middle of the plot, i.e. between 60 and 75 min. As residence time of the reactor increases, fixed capital cost of the process surges while favouring the BEC by increase the conversion of lipids. However, greater residence time results in the increased material inside the reactor, causing the increased IR. EI99 also increases because of the more utility consumption and steel usage in the reactor manufacturing.

Feed plate of distillation columns affect performance of all objectives. For FRAC-1, the feed plate lies near to the upper bound (Fig. 5d), which is near to reboiler, indicating the minimum steam duty and minimum reflux which is favourable for the all the objectives. Optimum feed plate for FRAC-2, FRAC-5, and FRAC-6 lie largely in the lower half (Figs. 5e, g, h). The feed plate of the DWC is scattered in middle (Fig. 5f) to minimize the steam consumption. Optimal points of LIQ-SPLIT-F4 lie in the upper half of the plot (Fig. 5i). Fig. 5(k) shows the optimal points for the VAP-SPLIT-F3; the optimum points are scattered between the upper and lower bounds. Both these variables affect the BEC, EI99, by minimizing the steam consumption in DWC. Fig. 5(k) shows the optimal COMP2-CR, which is found to be in lower portion of the plot (i.e. between 2.2 and 3.34). It is due to the fact that as the compression ratio increases, the capital cost as well as the electricity consumption of process also increases. This results in the increase of BEC and EI99. COMP2-CR does not influence IR significantly. Hence, minimum compression ratio is found to be favourable with respect of BEC and EI99. Similarly, OH-VAP-SPLIT (Fig. 5l) increases the vapor flow in the compressor, thereby causing the increased electricity consumption and internal flow into the column. Consequently, EI99 and IR of the process are negatively affected. Hence, a lower OH-VAP-SPLIT is favourable for minimization of these objectives. Fig. 6 shows the three-dimensional overview of the simultaneous optimization all three objectives. BEC increases from \$2.0 to \$4.5 per kg for the decrease in (a) IR from 2.2×10^{-5} to 1.4×10^{-5} per year and (b) EI99 from 21×10^5 to 12×10^5 points per year. Best point from the Pareto optimal curve, obtained from SAW method, corresponds to the BEC of \$2.47 per kg, IR of 1.62×10^{-5} per year and EI99 of 11.41×10^5 points. From Fig. 6, it can be seen that the BEC of the biodiesel can be reduced at the cost of increased EI99 and IR. Any attempt to decrease the IR of the process leads to the increased BEC (up to \$4.5 per kg) and EI99 (up to 21×10^5 points per year). This 3D graph is useful to the decision maker for the appropriate understanding of the relationship among the three objectives.

4.4. Simple additive weighting ranking method

Each point on the Pareto optimal front is the optimum design for a specific case. To select one solution from the front is a challenge for a decision maker. Different methods are available for the selection of the best solution from the large number of solutions. Wang and Rangaiah (2017) studied the performance of over ten ranking methods. On the basis of user input, applicability and simplicity of principle, Wang and Rangaiah (2017) reported that Simple Additive Weighting (SAW) method is a better ranking method for choosing best of the non-dominated optimal solution. SAW method is useful for the selection of best solution in case of MOO. SAW is often known as weighted linear combination or scoring approaches. For every alternative, a score is determined by multiplying the scaled value given to that attribute's alternative with the weights of relative importance assumed by the user, and then the results for all criteria are summed up (Afshari et al., 2010). The option with the highest score is treated as the best and is recommended.

$$F_{ij} = \frac{f_i^-}{f_{ij}} \quad \text{for minimization objective,} \quad \text{where} \quad f_j^- = Min_{i \in m} f_{ij} \tag{8}$$

Apply the weighted normalised objective matrix to create the weighted normalised objective matrix.

$$v_{ij} = F_{ij} \times w_j \tag{9}$$

Calculate the score of each optimal solution, which is the sum of

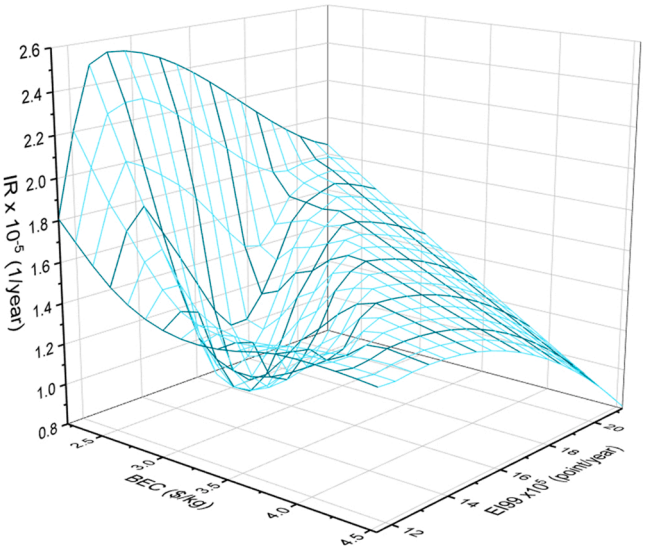

Fig. 6. Three-dimensional front of simultaneous MOO study of BEC, EI99, and IR.

weighted values,

$$A_i = \sum_{j=1}^{n} V_{ij} \quad (10)$$

Where, f_{ij}: i^{th} value of the j^{th} objective, F_{ij}: value of f_{ij} after normalization, v_{ij}: weighted value or rank of f_{ij} or F_{ij}, and w_j: weightage of the j^{th} objective, f_i^-: minimum value among the solutions. In this study, for the calculation of the first rank solution among all optimal solution, 50% weightage is given to each objective in bi-objective study and 30%, 30%, and 40% weightage is given to BEC, EI99 and IR, respectively. For each run, first rank solution was found out which is marked as 'Δ' in Fig. 3(a), 4(a), and 5(a).

4.5. Comparative analysis

To exemplify the benefit of MOO of retrofitted biodiesel process, a comparative analysis is conducted between the best solutions obtained using the SAW method. The comparison is presented in Table 4.

The best optimal points are marked as 'Δ' in Fig. 3(a) and Fig. 4(a), whereas, the optimal point can be identified by a 'Δ' mark in Fig. 5(a). For the Case A, the BEC of the process is reduced to \$1.85 from \$3.07 per kg (~39%), while EI99 for the process reduced to 21.10×10^5 from 22.17×10^5 points per year (~4%). In Case B, BEC of the process is reduced by 10.75% (from \$3.07 to \$2.74 per kg) with reduction in IR to 1.44×10^{-5} from 1.82×10^{-5} per year. Simultaneous minimization of all three objectives (Case C), BEC is reduced to \$2.47 per kg (~19.5%), EI99 is reduced to 11.49×10^5 points (~48%), and IR is reduced to $1.63 * 10^{-5}$ (10.4%) with respect to the values in the base case. Economics, environmental considerations and safety of the process are improved substantially by performing the MOO study using HMODE-DLS algorithm. This improvement is due to the optimum decision variable, namely reactor temperature, residence time, feed trays, LIQ-SPLIT-F4, VAP-SPLIT-F3, COMP2-CR and OH-VAP-SPLIT, all of which influence the objectives in different ways.

Table 5 shows the decision variables for the best/first rank Pareto optimal solution obtained using the SAW method. Case A yielded about 40% saving in BEC and about 5% savings in EI99. Case B depicted about 11% savings in BEC and about 21% savings in IR. Simultaneous minimization of all three objectives (Case C) resulted in significant decrease in BEC (~20%), EI99 (~48%) and IR (~10%). These saving are crucial as they denote economic, environmental, and safety benefits. Table 5 shows the variables employed in the base case and obtained through HMODE-DLS for the optimized cases. In general, higher residence time in the reactor (RTRANS in Fig. 1) is found to be beneficial. Feed trays largely stay near to the reboiler. Other decision variables, except reactor temperature, lie near to the values used in the base case. The cost of the microalgae lipid taken in this work is 0.065 \$/kg. At steady state, cost of microalgae lipid as raw material contributes to around 40% of the manufacturing cost. Hence, there is scope for decreasing the break-even cost of biodiesel by improving the cultivation and harvesting methodology. If the cost of manufacturing of microalgal lipid decreased, it will have a bearing on the reduction of the cost of biodiesel. In this work, lipid content in the microalgae is assumed to be 30% on dry basis and 5% on wet basis. There is scope to decrease the cost of biodiesel by increasing the lipid content in the microalgae. It is possible to increase lipid content in the microalgae by using advance techniques.

5. Conclusions

Ultrasound assisted, IL catalyzed, and DWC-MVR retrofitted in situ biodiesel production from wet microalgae is optimized considering three important criteria. Multiobjective optimization of BEC, EI99, and IR showed significant decrease in BEC (~20%), EI99 (~48%), and IR (~10%). The Pareto optimal fronts clearly depicted that BEC is reduced at the cost of IR and EI99. The rationale behind the obtained trade-offs between objectives are clearly contemplated in terms of the decision variables, in this study. The quantitative trade-offs between objectives facilitate better process design and operation while meeting multiple important constraints related to economics, environment, and safety. Process retrofitting using DWC-MVR may pose difficulty in controlling the process, which requires further investigation. Also, efforts should be devoted to reduce biodiesel breakeven cost by improving the lipid content in microalgae and overall efficiency of microalgal cultivation.

Table 4
Optimized processes and the base case comparison (BEC: \$/kg, EI99: points/year, IR: $year^{-1}$).

S. No.	Objectives	Base case	*MOO Cases* (% savings w.r.t. base case)		
			BEC and EI99 (Case A)	BEC and IR (Case B)	BEC, EI99, IR (Case C)
1	BEC (\$/kg)	3.07	1.85 ***(39.73%)***	2.74 ***(10.74%)***	2.47 ***(19.543%)***
2	EI99	2217518	2109255 ***(4.84%)***	–	1149265 ***(48%)***
3	IR (1/year)	$1.82 * 10^{-5}$	–	$1.44 * 10^{-5}$ **(20.8%)**	$1.63 * 10^{-5}$ **(10.43)**

Table 5
Comparison of decision variables in base case and in different optimized cases.

Sr. No.	Decision variable	*Cases*			
		Base case	BEC vs EI99 (Case A)	BEC vs IR (Case B)	BEC vs EI99 vs IR (Case C)
1	Temperature of reactor (°C)	45	43.47	38.19	59.60
2	Residence time of reactor (min)	60	83.91	74.42	70.25
3	(Feed Stage) $_{FRAC-1}$	4	6	5	6
4	(Feed Stage) $_{FRAC-2}$	8	9	9	9
5	(Feed Stage) $_{FRAC-3}$	5	4	6	4
6	(Feed Stage) $_{FRAC-5}$	7	8	6	6
7	(Feed Stage) $_{FRAC-6}$	6	8	8	8
8	LIQ-SPLIT-F4	366	323.6	326.7	384.57
9	VAP-SPLIT-F3	2460	2397	2430	2638
10	COMP2-CR	3.5	2.98	3.16	3.09
11	OH-VAP-SPLIT	0.5	0.64	0.48	0.68

Declaration of Competing Interest

The authors declare that they have no known competing financial interests or personal relationships that could have appeared to influence the work reported in this paper.

Acknowledgement

Authors thank Dr. Ashish Gujrathi (SQU Oman) for his guidance pertaining to HMODE algorithm.

Appendix A. Supporting information

Supplementary data associated with this article can be found in the online version at doi:10.1016/j.psep.2022.05.059.

References

Afshari, A., Mojahed, M., Yusuff, R.M., 2010. Simple additive weighting approach to personnel selection problem. Int. J. Innov. Manag. Technol. 1, 511–515.

Ahmed, M., Patle, D.S., Ahmad, Z., Abdullah, A., Rohman, F.S., 2020. Energy and economic analysis of in situ biodiesel production from microalgal biomass 97, 1762–1768.
AIChE, 2000. Guidelines for Chemical Process Quantitative Risk Analysis, Second edition. AIChE.
Akkarawatkhoosith, N., Srichai, A., Kaewchada, A., Ngamcharussrivichai, C., Jaree, A., 2019. Evaluation on safety and energy requirement of biodiesel production: conventional system and microreactors. Process Saf. Environ. Prot. 132, 294–302. https://doi.org/10.1016/j.psep.2019.10.018.
Alagumalai, A., Mahian, O., Hollmann, F., Zhang, W., 2021. Environmentally benign solid catalysts for sustainable biodiesel production: a critical review. Sci. Total Environ. 768, 144856 https://doi.org/10.1016/j.scitotenv.2020.144856.
Ananthi, V., Balaji, P., Sindhu, R., Kim, S.H., Pugazhendhi, A., Arun, A., 2021. A critical review on different harvesting techniques for algal based biodiesel production. Sci. Total Environ. 780, 146467 https://doi.org/10.1016/j.scitotenv.2021.146467.
Ani, A.Z., Gujarathi, A.M., Vakili-Nezhaad, G.R., Al-Muhtaseb, A.H., 2020. Hybridization Approach towards improving the performance of evolutionary algorithm. Arab. J. Sci. Eng. 45, 11065–11086. https://doi.org/10.1007/s13369-020-04964-y.
Ani, A.Z., Gujarathi, A.M., Vakili-Nezhaad, G., 2021a. Hybridized multi-objective optimization approach (HMODE) for lysine fed-batch fermentation process. Korean J. Chem. Eng. 38, 8–21. https://doi.org/10.1007/s11814-020-0642-y.
Ani, A.Z., Gujarathi, A.M., Vakili-Nezhaad, G.R., 2021b. Simultaneous energy and environment-based optimization and retrofit of TEG dehydration process: an industrial case study. Process Saf. Environ. Prot. 147, 972–984. https://doi.org/10.1016/j.psep.2021.01.018.
Ayub, H.M.U., Ahmed, A., Lam, S.S., Lee, J., Show, P.L., Park, Y.K., 2022. Sustainable valorization of algae biomass via thermochemical processing route: an overview. Bioresour. Technol. 344, 126399 https://doi.org/10.1016/j.biortech.2021.126399.
Barange, S.H., Raut, S.U., Bhansali, K.J., Balinge, K.R., Patle, D.S., Bhagat, P.R., 2021. Biodiesel production via esterification of oleic acid catalyzed by Brønsted acid-functionalized porphyrin grafted with benzimidazolium-based ionic liquid as an efficient photocatalyst. Biomass Convers. Biorefin. https://doi.org/10.1007/s13399-020-01242-7.
Chisti, Y., 2008. Biodiesel from microalgae beats bioethanol. Biotechnol. Adv. 25, 294–306. https://doi.org/10.1016/j.tibtech.2007.12.002.
Christophe, G., Kumar, V., Nouaille, R., Gaudet, G., Fontanille, P., Pandey, A., Socco, C. R., Larroche, C., 2012. Recent developments in microbial oils production: a possible alternative to vegetable oils for biodiesel without competition with human food? Braz. Arch. Biol. Technol. 55, 29–46. https://doi.org/10.1590/S1516-89132012000100004.
Contreras-Zarazúa, G., Sánchez-Ramírez, E., Vázquez-Castillo, J.A., Ponce-Ortega, J.M., Errico, M., Kiss, A.A., Segovia-Hernández, J.G., 2019. Inherently Safer Design and Optimization of Intensified Separation Processes for Furfural Production. Ind. Eng. Chem. Res. 58, 6105–6120. https://doi.org/10.1021/acs.iecr.8b03646.
Contreras-Zarazúa, G., Jasso-Villegas, M.E., Ramírez-Márquez, C., Sánchez-Ramírez, E., Vázquez-Castillo, J.A., Segovia-Hernandez, J.G., 2021. Design and intensification of distillation processes for furfural and co-products purification considering economic, environmental, safety and control issues. Chem. Eng. Process. - Process Intensif. 159 https://doi.org/10.1016/j.cep.2020.108218.
Crowl, D., A., Louvar, J., F., 2002. Chemical process safety fundamental with application (2nd Ed.), Prentice Hall International Series.
Deshmukh, S., Kumar, R., Bala, K., 2019. Microalgae biodiesel: A review on oil extraction, fatty acid composition, properties and effect on engine performance and emissions. Fuel Process. Technol. 191, 232–247. https://doi.org/10.1016/j.fuproc.2019.03.013.
Deshpande, G., Shrikhande, S., Sawarkar, A.N., Patle, D.S., 2022. Multiobjective optimization of ultrasound intensified and ionic liquid catalyzed in situ algal biodiesel production considering economic, environmental and safety indicators. Chem. Eng. Res. Des. 180, 134–152. https://doi.org/10.1016/j.cherd.2022.02.011.
Ganesan, R., Manigandan, S., Shanmugam, S., Chandramohan, V.P., Sindhu, R., Kim, S. H., Brindhadevi, K., Pugazhendhi, A., 2021. A detailed scrutinize on panorama of catalysts in biodiesel synthesis. Sci. Total Environ. 777, 145683 https://doi.org/10.1016/j.scitotenv.2021.145683.
Goedkoop, M.J., Spriensma, R., 2001. The Eco-indicator 99 - A damage oriented method for Life Cycle Impact Assessment. Assessment 144.
Gunawan, F., Kurniawan, A., Gunawan, I., Ju, Y.H., Ayucitra, A., Soetaredjo, F.E., Ismadji, S., 2014. Synthesis of biodiesel from vegetable oils wastewater sludge by in-situ subcritical methanol transesterification: Process evaluation and optimization. Biomass Bioenergy 69, 28–38. https://doi.org/10.1016/j.biombioe.2014.07.005.
Haag, U. de, Ale, B.J., 2005. Guidelines for Quantitative Risk Assessment 2nd ed. Netherlands Organ. Delft, Netherlands. ⟨https://doi.org/10.26634/jfet.6.1.1292⟩.
Heo, H.Y., Heo, S., Lee, J.H., 2019. Comparative techno-economic analysis of transesterification technologies for microalgal biodiesel production. Ind. Eng. Chem. Res. 58, 18772–18779. https://doi.org/10.1021/acs.iecr.9b03994.
Karmakar, B., Halder, G., 2019. Progress and future of biodiesel synthesis: advancements in oil extraction and conversion technologies. Energy Convers. Manag. 182, 307–339. https://doi.org/10.1016/j.enconman.2018.12.066.
Khiratkar, A.G., Balinge, K.R., Patle, D.S., Krishnamurthy, M., Cheralathan, K.K., Bhagat, P.R., 2018. Trasaesterification of castor oil using benzimidazolium based Bronsted acid ionic liquid catalyst. Fuel 231, 458–467.
Kumar, V., Kiran, B., Jana, A.K., Samanta, A.N., 2012. A novel multistage vapor recompression reactive distillation system with intermediate reboilers. AIChE J. 59, 761–771.
Luyben, W.L., 2002. Plantwide Dynamic Simulators in Chemical Processing and Control. CRC Press.
Marler, R.T., Arora, J.S., 2010. The weighted sum method for multi-objective optimization: new insights. Struct. Multidisc. Optim. 853–862. https://doi.org/10.1007/s00158-009-0460-7.
Martinez-Gomez, J., Sanchez-Ramirez, E., Quiroz-Ramirez, J.J., Segovia-Hernandez, J. G., Ponce-Ortega, J.M., El-Halwagi, M.M., 2016. Involving economic, environmental and safety issues in the optimal purification of biobutanol. Process Saf. Environ. Prot. 103, 365–376.
Mathew, G.M., Raina, D., Narisetty, V., Kumar, V., Saran, S., Pugazhendi, A., Sindhu, R., Pandey, A., Binod, P., 2021. Recent advances in biodiesel production: challenges and solutions. Sci. Total Environ. 794, 148751 https://doi.org/10.1016/j.scitotenv.2021.148751.
Medina-Herrera, N., Jiménez-Gutiérrez, A., Mannan, M.S., 2014. Development of inherently safer distillation systems. J. Loss Prev. Process Ind. 29, 225–239. https://doi.org/10.1016/j.jlp.2014.03.004.
Milbrandt, A., Jarvis, E., 2010. Resource evaluation and site selection for microalgae production in India. Engineering 123–203.
Mustapha, S.I., Bux, F., Isa, Y.M., 2021. Techno-economic analysis of biodiesel production over lipid extracted algae derived catalyst. Biofuels 0, 1–12. https://doi.org/10.1080/17597269.2021.1878577.
Ong, H.C., Tiong, Y.W., Goh, B.H.H., Gan, Y.Y., Mofijur, M., Fattah, I.M.R., Chong, C.T., Alam, M.A., Lee, H.V., Silitonga, A.S., Mahlia, T.M.I., 2021. Recent advances in biodiesel production from agricultural products and microalgae using ionic liquids: opportunities and challenges. Energy Convers. Manag 228. https://doi.org/10.1016/j.enconman.2020.113647.
Patle, D.S., Sharma, S., Ahmad, Z., Rangaiah, G.P., 2014. Multi-objective optimization of two alkali catalyzed processes for biodiesel from waste cooking oil. Energy Convers. Manag 85, 361–372. https://doi.org/10.1016/j.enconman.2014.05.034.
Patle, D.S., Sharma, S., Gadhamsetti, A.P., Balinge, K.R., Bhagat, P.R., Pandit, S., Kumar, S., 2018. Ultrasonication-assisted and benzimidazolium-based brønsted acid ionic liquid-catalyzed transesterification of castor oil. ACS Omega 3, 15455–15463. https://doi.org/10.1021/acsomega.8b02021.
Patle, D.S., Shrikhande, S., Rangaiah, G.P., 2020. Process development, design and analysis of microalgal biodiesel production aided by microwave and ultrasonication. Process Syst. Eng. Biofuels Dev. 2030, 259–284. https://doi.org/10.1002/9781119582694.ch10.
Patle, D.S., Pandey, A., Srivastava, S., Sawarkar, A.N., Kumar, S., 2021. Ultrasound-intensified biodiesel production from algal biomass: a review. Environ. Chem. Lett. 19, 209–229. https://doi.org/10.1007/s10311-020-01080-z.
Piemonte, V., Di Paola, L., Iaquaniello, G., Prisciandaro, M., 2016. Biodiesel production from microalgae: ionic liquid process simulation. J. Clean. Prod. 111, 62–68. https://doi.org/10.1016/j.jclepro.2015.07.089.
Pukale, D.D., Maddikeri, G.L., Gogate, P.R., Pandit, A.B., Pratap, A.P., 2015. Ultrasound assisted transesterification of waste cooking oil using heterogeneous solid catalyst. Ultrason. Sonochem. 22, 278–286. https://doi.org/10.1016/j.ultsonch.2014.05.020.
Ramírez-Márquez, C., Contreras-Zarazúa, G., Martín, M., Segovia-Hernández, J.G., 2019. Safety, economic, and environmental optimization applied to three processes for the production of solar-grade silicon. ACS Sustain. Chem. Eng. 7, 5355–5366. https://doi.org/10.1021/acssuschemeng.8b06375.
Rastogi, R.P., Pandey, A., Larroche, C., Madamwar, D., 2018. Algal green energy – R&D and technological perspectives for biodiesel production. Renew. Sustain. Energy Rev. 82, 2946–2969. https://doi.org/10.1016/j.rser.2017.10.038.
Sánchez-Ramírez, E., Hernandez, J.J.Q.-R.S., Segovia-Hernandez, J.G., Kiss, A.A., 2017. Optimal hybrid separations for intensified downstream processing of biobutanol. Sep. Purif. Technol. 185, 149–159. https://doi.org/10.1016/j.seppur.2017.05.011.
Sawarkar, A.N., 2019. Cavitation induced upgrading of heavy oil and bottom-of-the-barrel: a review. Ultrason. Sonochem. 58, 104690 https://doi.org/10.1016/j.ultsonch.2019.104690.
Sharma, S., Rangaiah, G.P., 2013. Multi-objective optimization of a bio-diesel production process. Fuel 103, 269–277.
Shrikhande, S., Deshpande, G., Sawarkar, A.N., Ahmad, Z., Patle, D.S., 2021. Chemical engineering research and design and retrofitting of ultrasound intensified and ionic liquid catalyzed in situ algal biodiesel production. Chem. Eng. Res. Des. 171, 168–185. https://doi.org/10.1016/j.cherd.2021.05.010.
Sivaramakrishnan, R., Incharoensakdi, A., 2017. Microalgae as feedstock for biodiesel production under ultrasound treatment – a review. Bioresour. Technol. 250, 877–887.
Sivaramakrishnan, R., Muthukumar, K., 2012. Isolation of thermo-stable and solvent-tolerant Bacillus sp. lipase for the production of biodiesel. Appl. Biochem. Biotechnol. 166, 1095–1111. https://doi.org/10.1007/s12010-011-9497-3.
Suganya, T., Kasirajan, R., Renganathan, S., 2014. Ultrasound-enhanced rapid in situ transesterification of marine macroalgae Enteromorpha compressa for biodiesel production. Bioresour. Technol. 156, 283–290. https://doi.org/10.1016/j.biortech.2014.01.050.
Thafseer, M., Al Ani, Z., Gujarathi, A.M., Vakili-Nezhaad, G.R., 2021. Towards process, environment and economic based criteria for multi-objective optimization of industrial acid gas removal process. J. Nat. Gas Sci. Eng. 88, 103800 https://doi.org/10.1016/j.jngse.2021.103800.
Tikadar, D., Gujarathi, A.M., Guria, C., 2021a. Safety, economics, environment and energy based criteria towards multi-objective optimization of natural gas sweetening process: an industrial case study. J. Nat. Gas Sci. Eng. 95, 104207 https://doi.org/10.1016/j.jngse.2021.104207.
Tikadar, D., Gujarathi, A.M., Guria, C., Al Toobi, S., 2021b. Retrofitting and simultaneous multi-criteria optimization with enhanced performance of an industrial gas-cleaning plant using economic, process safety, and environmental objectives. J. Clean. Prod. 319, 128652 https://doi.org/10.1016/j.jclepro.2021.128652.

Turton, R., Bailie, R.C., Whiting, W.B., Shaeiwitz, J.A., 2008. Analysis, Design and Synthesis of Chemical Processes.

Wang, Z., Rangaiah, G.P., 2017. Application and analysis of methods for selecting an optimal solution from the pareto-optimal front obtained by multiobjective optimization. Ind. Eng. Chem. Res. 56, 560–574. https://doi.org/10.1021/acs.iecr.6b03453.

Xu, L., Li, M., Yin, X., Yuan, X., 2017. New intensified heat integration of vapor recompression assisted dividing wall column. Ind. Eng. Chem. Res. 56, 2188–2196. https://doi.org/10.1021/acs.iecr.6b03802.